was used; 16 transients were taken for each t_1 increment, and the total measuring time was 8.6 h. The 1K × 4K transform required ca. 3 h.

NOE 2-D Spectrum. The pulse sequence $90°-t_1/2-90°-\tau_m-90°-t_1/2-\mathrm{FID}(t_2)$ was used with a randomized[20] mixing time of 1 s. The data were treated as described for the SECSY spectrum; 16 transients were taken for each t_1 increment, and the total measuring time was 11.5 h. The 1K × 4K transform required ca. 3 h. In this experiment with three pulses a 16-phase cycle is not sufficient to eliminate quadrature image signals, which appear on a line of slope $^1/_2$ intersecting the $\omega_1 = 0$ axis at $\omega_2 = 0$ (the position of the RF carrier for quadrature detection). The line of image peaks is denoted by arrows in Figure 8.

Acknowledgment. We thank the Deutsche Forschungsgemeinschaft and the Fonds der Chemischen Industrie for financial support.

Registry No. 1d, 83174-89-4; **2d**, 83199-50-2; BOC-(α-^{2}H)-D,L-Pro-L-Pro$_2$-OTcp, 83174-88-3; *cyclo*-(L-Pro$_2$-D-Pro), 70493-40-2.

Optical vs. Thermodynamic Basicities: Probe Pb^{2+} Ion Spectra in Thermodynamically Characterized Molten Chloroaluminate Solutions

C. A. Angell* and P. D. Bennett[1]

Contribution from the Department of Chemistry, Purdue University, West Lafayette, Indiana 47907. *Received April 30, 1982*

Abstract: The energy of the outer-shell $^3P_1 \leftarrow {}^1S_0$ transition of Pb^{2+} doped into various binary chloroaluminate solutions has been studied in an attempt to gain insight into the changes in electronic states of anions in a binary chloride solution state as the composition is changed through a region of abrupt thermodynamic changes (equivalence point). Sudden shifts in the band maximum of as much as 3000 cm^{-1} are observed to occur at the stoichiometry of $AlCl_4^-$, the range over which the change occurs closely matching the 0.5 mol % wide region of rapid chloride activity change observed in earlier measurements. In the case of the low-melting system $AlCl_3$ + ethylammonium chloride, spectra were taken at 0.05 mol % intervals at 90 °C and it was noted that the entire energy shift occurred across a 0.2 mol % gap in which the Pb^{2+} was quantitatively rejected from solution (presumably as $PbCl_2$ although $Pb(AlCl_4)_2$ has not been excluded). In this case a second composition region of spectral shift was found that corresponds with one in which NMR studies in a related system also indicate a second acid-base process. The correlation with thermodynamically determined basicity changes in these systems is good enough to justify the use of Pb^{2+} as a basicity indicator and to lend credence to the optical basicity scale proposed on the basis of the nephelauxetic effect for $d^{10}s^2$ cations in acid media. However, measurements to be reported separately on the isoelectronic Tl^+ and Bi^{3+} spectra in the same systems show that caution is necessary. An ion in this series will only be an effective and reliable indicator for basicity changes if, as for aqueous acid-base indicators, it is approximately midway in basicity between the acidic and basic species being reacted.

Introduction

The basic chemical study described in this paper has been motivated by a need to resolve a problem impeding the development of an understanding of physical processes in technically important inorganic glasses. It has been known for a long time that structural features of ionic liquids and glasses such as the coordination number of a transition-metal ion, and chemical features such as oxidation states, are strongly dependent on what is loosely referred to as the "basicity" of the glass.[2] However, it has only recently been realized that important dynamic properties such as the electrical conductivity are also closely related to the same quantity.[3] Given the current surge of interest in glasses as fast ion solid electrolytes, it is now more important than ever that means of quantifying the concepts involved in the terms "basicity" and "oxide ion activity", and in particular of making comparisons between systems of quite different composition, be developed.

For individual liquid binary systems, the "basicity" can be defined quite precisely in terms of the thermodynamic activity of the more basic component as determined by, e.g., electrochemical or conventional vapor pressure methods. Although such measurements are not simple in hot corrosive liquids, they have been performed in limited composition ranges in such fundamental systems as $Na_2O + SiO_2$. In this system a_{Na_2O} ($=a_\pm^2$) has been widely studied in both liquid and vitreous states. However, if a comparison of physical or chemical behavior in two different binary systems, e.g., $Na_2O + SiO_2$ and $Li_2O + GeO_2$, is desired, thermodynamics is limited in its ability to help, even though it seems clear that the differences in behavior observed have much to do with the quantity conceptualized, but not quantified, as "basicity" or "oxide ion activity". The best that can be done is to probe each system with a test species whose activity would be measured.

Another problem is raised on passing to the glassy state, in which thermodynamic equilibrium is not maintained. Due to the mobility of certain components of the glass structure, electrochemical measurements can still be performed and variations of chemical potential with composition can be measured,[3] but their precise relation to the corresponding liquid-state properties is clouded, particularly when the glass transition temperature T_g is highly composition dependent.

In view of these problems it is of interest to develop nonthermodynamic probes of the chemical state of the liquid or glass, probes that are sensitive to the states of chemical binding or polarization of the ionic or quasi-ionic components of the system, which, after all, determine the thermodynamic activities under discussion. Such probes will be most helpful if their behavior can be shown to exhibit the same response to composition changes as does the thermodynamic basicity or some suitable function of it.

(1) Present address: Standard Oil of Ohio, Cleveland, OH 44115.

(2) Detailed reviews and analysis of this problem area are given in: (a) J. Wong and C. A. Angell, "Glass: Structure by Spectroscopy", Marcel Dekker, New York, 1976; (b) C. A. Angell in "Spectroscopic and Electrochemical Characterization of Solute Species in Non-Aqueous Solutions", G. Mamantov, Ed., Plenum Press, New York, 1977, p 273.

(3) (a) D. Ravaine and J. L. Souquet, *Phys. Chem. Glasses*, **18**, 27 (1977); (b) D. Ravaine, *J. Non-Cryst. Solids*, **38-39**, 353 (1980); (c) J. L. Souquet, *Solid State Ionics*, in press.

0002-7863/82/1504-6304$01.25/0

With this object in mind, and with the encouragement of the success that Duffy and Ingram have had with their formulation and application of the "optical basicity" concept,[4a] we have undertaken a study of the spectroscopy of $d^{10}s^2$ cations in acid–base systems which are experimentally tractable and in which the thermodynamic properties are well-known.

The outer-orbital $^3P_1 \leftarrow {}^1S_0$ ("Rydberg") transitions of $d^{10}s^2$ cations are unusually sensitive to the electron-donating propensity of the ligands with which they coordinate. These spectral responses have been studied many times previously in crystals[4b,5,6] and glasses[6-15] and in some isolated examples of molten salts also.[10,16] The most broadly based investigations have been those of Duffy and Ingram,[8-13] who have shown that the spectral shifts are more or less systematic in the electron-donating capacity of the average ligand. For instance, all three $6d^{10}6s^2$ probe ions Tl^+, Pb^{2+}, and Bi^{3+} exhibit progressive "red" shifts, not only with increasing base concentration within a single system (e.g., $Na_2O + B_2O_3$) but also as the Cl^- to SO_4^{2-} ratio is systematically increased by appropriate composition changes within the system $ZnCl_2$–KCl–K_2SO_4.[11] The shift corresponds to increased inner-shell shielding (due to ligand electron donation) of the outer-orbital structure within which the observed Rydberg transitions occur.

On the basis of these observations, Duffy and Ingram proposed[10] to use the spectral shifts as a means of quantifying the concept of Lewis basicity, which, though broadly applied, has always lacked a numerical scale. The proposed "optical basicity" scale is based on Jørgensen's analysis[17] of the nephelauxetic effect for first-row transition-metal ions, and is defined by

$$\Lambda = \frac{\nu_f - \nu}{\nu_f - \nu_{min}} \quad (1)$$

where Λ is the optical basicity, ν_f is the frequency of the $^3P_1 \leftarrow {}^1S_0$ transition of the free probe ion (obtained by extrapolation to $h = 0$, where h is the Jørgensen h function for the ligands of various host media[9]), ν is the transition frequency in the particular solvent system, and for an all-oxide system, $\nu_{min} = \nu_{O^{2-}}$ determined separately in an "ionic" or "free donor" oxide. For a chloride system $\nu_{min} = \nu_{Cl^-}$ determined in the most ionic chloride system available. Since there is not "ideal" free donor state to complement the "free ion" value of ν, an element of arbitrariness enters the scale in the choice of ν_{min}.

In combination with a simple scheme, based on Pauling electronegativities, for predicting the values of the optical basicity for previously unstudied solvent systems, Duffy and Ingram have had considerable success in applying this concept to the interpretations of oxide glass chemistry. This had led them to restate the Lux–Flood acid–base concept[19,20] for application in glass chemistry as follows: "An acid–base reaction in an oxyanion glass is one in which oxide ions change from one state of (optical) basicity to another."[4a]

An obvious question that has not yet been properly answered is the following: How closely does the optical basicity of a chosen glassy system defined by eq 1 follow the thermodynamic basicity defined by the activity of the basic component, e.g., of Na_2O in the binary system $Na_2O + SiO_2$ (or, more appropriately, log a_{Na_2O})? A desirable way to test this would be to monitor the optical basicity in an oxide glass as a function of composition in a range where large changes in activity of the basic oxide are known to occur, e.g., across the orthophosphate or orthosilicate composition ranges in the respective binary systems $P_2O_5 + Na_2O$ and $SiO_2 + Na_2O$. Rapid changes in Λ have indeed been observed by Duffy and Ingram[12] at the metaphosphate stoichiometry in the former system, and similar breaks have been noted in borate glasses by Klein and Oronato,[13] where nonbridging oxygens are believed to first appear. However, these are not as pronounced or as abrupt as would be expected at the primary equivalence points where free oxide ion first appears, and many orders of magnitude change in alkali oxide activity would be expected. Unfortunately, the liquid states of oxides at these latter (orthosilicate, orthophosphate) stoichiometries are not easy to study due to high temperature and severe corrosion problems. Furthermore, precise liquid-state thermodynamic data in the region of the equivalence point are not available. Thus the basicity relationships cannot easily be determined in oxide systems. However, a parallel neutralization process occurs in some low-melting noncorrosive molten chloride systems where the chloride ion activity is known to change many orders of magnitude with small changes in melt composition. These melts are therefore well suited to the study of this problem.

This paper is primarily aimed at an evaluation of the relationship between spectral shifts (implying optical basicity) and thermodynamic basicity, utilizing the known values of the latter,[22-24] in $AlCl_3$–alkali chloride systems. The activity of the alkali chloride in these solutions changes by some 6–8 orders of magnitude at the equivalence point. We have included one low-temperature system, $AlCl_3$ + ethylammonium chloride (abbreviated (EAH)Cl), which combines spectroscopic transparency in the near-UV region with ease of handling and exceptional basicity range. It is also glass forming on both sides of the tetrachloroaluminate stoichiometry, though specific use has not been made of this property in our investigation.

Experimental Section

Materials Purification. Reagent grade NaCl and KCl were recrystallized twice by slowly cooling, over a period of 2–3 days, a saturated aqueous solution of each of these salts. Large NaCl and KCl crystals were grown in this manner. The crystals were dried in vacuo at a temperature of 140 °C for at least 24 h. For ease of handling, small beads, ranging in size from 0.5 to 2 mm in diameter, were made by dripping the molten salt through a quartz capillary into liquid nitrogen.

Ethylammonium chloride ((EAH)Cl) beads were made similarly with reagent grade (EAH)Cl that had been recrystallized from acetonitrile and dried at 100 °C. (EAH)Cl undergoes a solid–solid transition at 85 °C, which produces a large enthalpy change and probably involves a rotational disordering of the $CH_3CH_2NH_3^+$ ions. The melting point of (EAH)Cl was found by differential scanning calorimetry (Perkin-Elmer DSC-2) to be 111 °C. The highest value reported in the literature[26,27] is 109 °C. A subsequent microanalysis showed the compound to have the stoichiometric quantities of each element to ±0.25%.

$AlCl_3$ for use in phase diagram determination and spectral studies was prepared by a distillation procedure essentially as described in the next section.

(4) (a) J. A. Duffy and M. D. Ingram, *J. Non-Cryst. Solids*, **21**, 373 (1976); (b) F. Seitz, *J. Chem. Phys.*, **6**, 150 (1938).
(5) D. S. McClure, *Solid State Phys.*, **9**, 512 (1959).
(6) A. K. Ghosh, *J. Chem. Phys.*, **42**, 2623 (1964); **44**, 535 (1966).
(7) (a) R. Reisfeld, *Struct. Bonding (Berlin)*, **13**, 53 (1973); (b) R. Reisfeld and L. Boehm, *J. Non-Cryst. Solids*, **16**, 83 (1974); **17**, 209 (1975); (c) R. Reisfeld, L. Boehm, and B. Barnett, *J. Solid State Chem.*, **15**, 140 (1975).
(8) J. A. Duffy and M. D. Ingram, *J. Chem. Soc. A*, 451 (1970).
(9) J. A. Duffy and M. D. Ingram, *J. Chem. Phys.*, **52**, 3752 (1970); **54**, 443 (1971).
(10) J. A. Duffy and M. D. Ingram, *J. Am. Chem. Soc.*, **93**, 6448 (1971).
(11) J. A. Duffy and M. D. Ingram, *J. Inorg. Nucl. Chem.*, **36**, 43 (1974); **37**, 1203 (1975).
(12) J. A. Duffy and M. D. Ingram, *Phys. Chem. Glasses*, **16**, 124 (1975).
(13) R. Klein and P. I. K. Onorato, *Phys. Chem. Glasses*, **21**, 199 (1980).
(14) A. Paul, *Phys. Chem. Glasses*, **11**, 46 (1970).
(15) A. Paul, *Phys. Chem. Glasses*, **13**, 144 (1972).
(16) G. P. Smith, D. W. James, and C. R. Boston, *J. Chem. Phys.*, **42**, 2249 (1965).
(17) C. K. Jørgensen, "Absorption Spectra and Chemical Bonding in Complexes", Pergammon Press, New York, 1962, pp 185–187.
(18) J. A. Duffy and M. D. Ingram, *Inorg. Chim. Acta*, **7**, 594 (1973).
(19) H. Lux, *Z. Electrochem. Angew. Phys. Chem.*, **45**, 303 (1934).
(20) H. Flood and T. Forland, *Acta Chem. Scand.*, **1**, 592 (1947).
(21) J. Shuppert and C. A. Angell, *J. Chem. Phys.*, **67**, 3050 (1977).
(22) G. Torsi and G. Mamantov, *Inorg. Chem.*, **10**, 1900 (1971); **11**, 1439 (1972).
(23) L. G. Boxall, H. L. Jones, and R. A. Osteryoung, *J. Electrochem. Soc.*, **12**, 223 (1973).
(24) L. G. Boxall, H. L. Jones, and R. A. Osteryoung, *J. Electrochem. Soc.*, **11**, 1439 (1972).
(25) P. B. Breckke, J. H. von Barner, and N. J. Bjerrum, *Inorg. Chem.*, **18**, 1372 (1979).
(26) A. Kisza and J. Hawronek, *Z. Phys. Chem. (Leipzig)*, **237**, 210 (1968).
(27) H. Hille, *J. Prakt. Chem.*, **64**, 401 (1901).

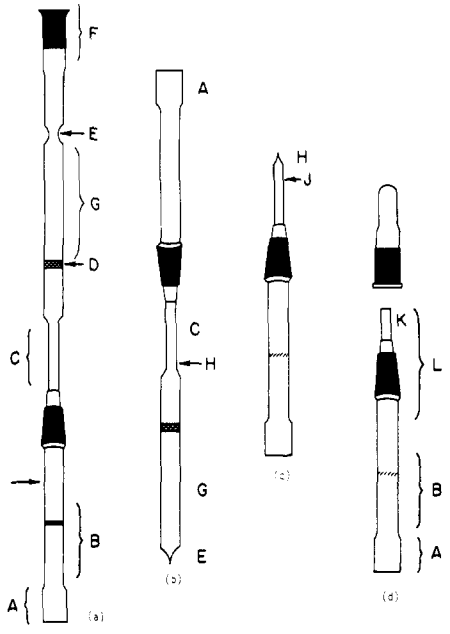

Figure 1. Glass constructions used in different stages of $AlCl_3$ + alkali chloride solution preparation for spectroscopic study. See text for explanation.

UV Spectroscopy Sample Preparation. Preparation of UV-transparent chloroaluminate solutions is a major problem due to the very difficult nature of $AlCl_3$. It was found convenient to make the purification and cell-filling steps an integral procedure.

First, a small quantity (~0.1 mol %) of $Pb(NO_3)_2$ was added by evaporation of an aqueous solution of known concentration to the cell section A–B of Figure 1a, which was initially separated from section C–F at the arrow. After A–B was joined to section C–F and oven dried, in vacuo, the cell was transferred to a 2 ppm water drybox and ~4 g of reagent grade $AlCl_3$, and Al metal strip, and a small NaCl crystal were added to section G. The frit D prevented the added materials from entering into the carefully cleaned spectrophotometric quartz cell (section A). The cell was stoppered and transferred to a vacuum line with a liquid nitrogen presample trap, evacuated to ~10^{-3} mmHg, and finally sealed at point E.

The cell was inverted and placed in a vertical tube furnace with section A–C uppermost and projecting (see Figure 1b); sufficient $AlCl_3$ was sublimed through frit D into section C to block the tube at H. This allowed the pressure to rise above the vapor pressure of liquid $AlCl_3$ at its melting point (~2.5 atm), thus causing the remaining $AlCl_3$ in section G to fuse. A small amount of liquid $NaAl_2Cl_7$ separated as a separate phase which scavenges most colorizing impurities (cf. Gale and Osteryoung[28]). The cell was then lowered into the furnace until only the cell section A remained exposed. Heating at point H released the $AlCl_3$ plug, and pure $AlCl_3$ was sublimed until ~3 g had collected in the cell. Section A–C was then separated by sealing off at H.

The cell, now in the configuration shown in Figure 1c, was heated to fuse the $AlCl_3$, and the volume of liquid was estimated to ±0.25 mL from a previous calibration of the cell section. From the known density, this yielded the mass of $AlCl_3$ to an accuracy, ±0.3 g, sufficient to locate to ±5% the composition of a binary solution after addition of a known quantity of second component in the next step. The exact composition is determined at the end of the experiment.

The cell was transferred to the drybox and broken open at J, and a calculated mass of NaCl, KCl, or (EAH)Cl beads was added to give a binary composition of ~53 mol % $AlCl_3$. For NaCl and KCl solutions the cell was then successively stoppered, (see Figure 1d), evacuated, and resealed at K so that the slow dissolution of NaCl or KCl would be carried out at $T > 300$ °C without loss of $AlCl_3$. For (EAH)Cl, air gun heating of the stoppered cell, Figure 1d, sufficed.

Titrations. After a homogeneous liquid was formed, the cell, again in a configuration similar to that in Figure 1c (for the $AlCl_3$–alkali chloride systems), was broken open just below the sealed portion and stoppered. Composition changes could then be made by adding preweighed salt beads to the cell now in the configuration of Figure 1d.

The precise composition of the final solution was determined at the end of the spectral titration by weighing before and after dissolution of the total sample to obtain, by difference, the imprecisely known $AlCl_3$ content.

Although the above "all-internal" procedure had the advantage of unfailingly producing the water-clear transparent melts essential to UV spectroscopy, the composition uncertainty while titrations were in process was a major deterrent to detailed study of the equivalence region. For the case of (EAH)Cl solutions, in which lower melt temperatures meant fewer colorization or vaporization problems, solutions containing 51 mol % $AlCl_3$ were successfully prepared by starting with weighed prepurified $AlCl_3$ and (EAH)Cl. Composition changes in steps of 0.05 mol % (EAH)Cl could then be made by addition of small preweighed (EAH)Cl beads.

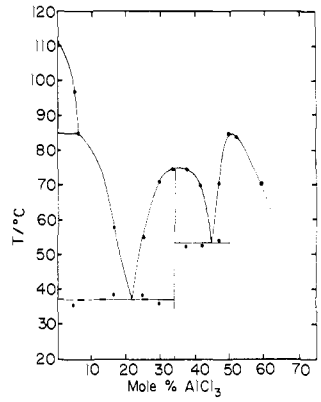

Figure 2. Phase diagram for the system ethylammonium chloride (EAH)Cl + aluminum chloride. The region above 60 mol % $AlCl_3$ was not studied in this work.

Spectrophotometric Arrangements. The optical cells were made from either square or rectangular quartz tubing, (A in Figure 1d) of path length 10 or 5 mm, respectively. They were fused via a graded seal B to a Pyrex upper compartment (section L, Figure 1d).

The absorption spectra were measured in the UV region of the spectrum with a Cary 14 spectrophotometer. An insulated aluminum block, fitting the sample compartment of the spectrophotometer, was used as a heater for the molten salts. The heater block featured a horizontal slot, through which the UV light could pass. Because the temperature dependence of the UV spectrum is weak, temperature control was not critical, and the ±3 °C obtainable with a Variac setting was quite adequate. The block temperature was monitored by an Omega Engineeric Model 175 digital thermometer (±1 °C accuracy). Since heat transfer to the sample was efficient and losses were small, the temperature of the melt could be assumed to be that of the heating block to within ±1 °C.

Phase Diagram Determination. For phase diagram study UV transparency was not required and fewer preparation problems had to be faced. Solutions were prepared by mixing weighed quantities of dry $AlCl_3$ and (EAH)Cl in a drybox and transferring 20-mg samples to aluminum DSC pans, which were then hermetically sealed. Solutions were fused and then cooled slowly in the DSC instrument to ensure complete crystallization. Thermal arrests or slope changes, which signal eutectic points and liquidus points, respectively, were determined during heating runs at 10 °C min^{-1}.

Results

Phase Diagram. $AlCl_3$ + Ethylammonium Chloride. The $AlCl_3$ + (EAH)Cl phase diagram determined in this study is shown in Figure 2. It is characterized by two congruently melting compounds at 33% $AlCl_3$ (T_m = 75 °C) and 50% $AlCl_3$ (T_m = 85 °C) and two eutectics at 22% $AlCl_3$ (T_E = 37 °C) and 45% $AlCl_3$ (T_E = 53 °C). A third eutectic presumably exists in the range 60–75% $AlCl_3$ and falls below room temperature. The origin of the compound at 33% $AlCl_3$ is believed to be the same for the corresponding compounds in the $AlCl_3$ + pyridinium chloride and $AlCl_3$ + α-picolinium chloride systems,[29] in which there is evidence for the H-bonded cation $[pyHClHpy]^+$.[30]

Spectra of Pb^{2+} in $AlCl_3$ and (EAH)Cl. The absorption spectrum of ~10^{-4} M Pb^{2+} in fused $AlCl_3$ at T = 230 °C is shown in Figure 3. It is characterized by a peak at λ_{max} = 258 nm (38 800 cm^{-1}) with full width at half-maximum (fwhm) 3710 cm^{-1}.

(28) R. J. Gale and R. A. Osteryoung, *Inorg. Chem.*, **18**, 1603 (1979).

(29) C. A. Angell, I. M. Hodge, and P. A. Cheeseman in "Molten Salts", J. P. Pemsler, Ed., The Electrochemical Society, London, 1976, p 138.

(30) J. W. Shuppert and C. A. Angell, *J. Phys. Chem.*, **84**, 538 (1980).

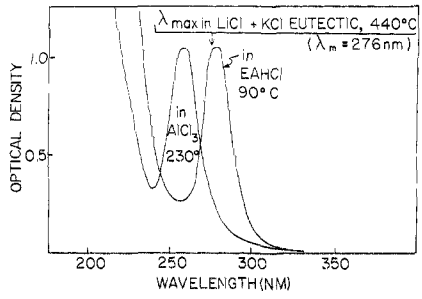

Figure 3. UV absorptions of Pb^{2+} in pure $AlCl_3$ and pure ethylammonium chloride due to the transition $^3P_1 \leftarrow {}^1S_0$. The position of the peak maximum in molten LiCl–KCl eutectic at 440 °C is indicated by the arrow.

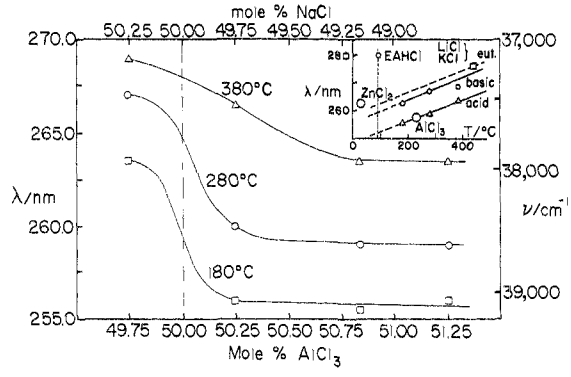

Figure 4. Variation of the Pb^{2+} UV absorption band maximum with composition in the system NaCl + $AlCl_3$ at different temperatures. The insert shows the peak position in relation to temperature on the acidic and basic sides of the equivalence point in the NaCl + $AlCl_3$ system. Peak positions for Pb^{2+} in other chloride environments at different temperatures are shown for comparison.

In fused (EAH)Cl at T = 90 °C, shown also in Figure 3, Pb^{2+} gives a spectrum that is characterized by a λ_{max} = 280 nm (35 700 cm^{-1}) and fwhm = 2660 cm^{-1}. For comparison purposes, the absorption spectrum of Pb^{2+} in the LiCl–KCl eutectic melt (41 mol % LiCl) at T = 440 °C, obtained by Smith et al.,[16] has λ_{max} = 276 nm (36 200 cm^{-1}) (see arrow in Figure 3) and fwhm = 3870 cm^{-1}. Background spectra of both pure fused $AlCl_3$ and (EAH)Cl showed no absorption in the region of interest.

Spectroscopic Titrations. Temperature Dependence. Figure 4 shows the position of the absorption band maximum (in wavelength units) as $AlCl_3$ is titrated with NaCl through the equivalence point at three temperatures. The solution is saturated at 50.3% NaCl at 180 °C. When the temperature is increased the following are observed: (i) the abruptness of the titration curve diminishes; (ii) the position of the absorption band at a given composition shifts toward lower energies by approximately 550 cm^{-1} for each 100 °C increase; (iii) the half-width (fwhm) increases.

Spectroscopic Titrations. Base Dependence. The variation of the band maximum with mole percent of base is compared for the bases NaCl and KCl in Figure 5. For KCl a somewhat greater mole percent excess of base can be added before saturation occurs, and it is found that the band position stays constant on either side of the equivalence point (unlike the case of $AlCl_3$ + (EAH)Cl; see below). The titrations were carried out at temperatures differing by 10 °C, an interval sufficient to change the band maximum by an increment outside the average experimental uncertainty; thus a third plot (dashed line) is shown correcting the NaCl titration plot to 270 °C. Note that from a common base on the $AlCl_3$-rich side, the spectral shift across the equivalence point is greater for the KCl titration ($\Delta\nu$ = 1600 vs. 1160 cm^{-1} for NaCl).

In the case of (EAH)Cl titrations a much wider range of compositions, extending to pure (EAH)Cl, can be explored. Results at 90 °C are shown in Figure 6 together with a plot for

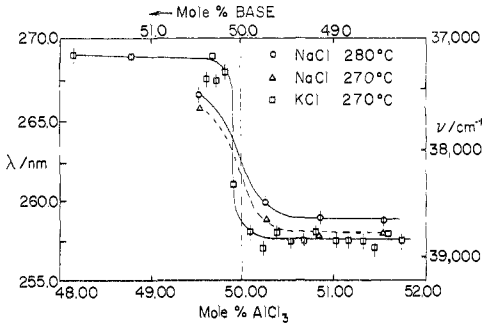

Figure 5. Variation of the Pb^{2+} band maximum with percent added base for the systems $AlCl_3$ + NaCl and $AlCl_3$ + KCl. The dashed line corrects the position of the curve for NaCl additions to the temperature of the curve for KCl additions. Note the greater shift in band maximum energy across the equivalence point for the KCl solutions.

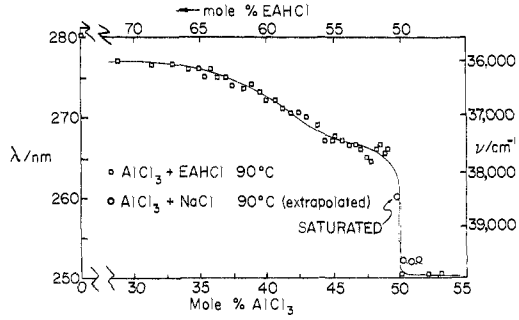

Figure 6. Dependence of the UV absorption maximum for Pb^{2+} in the system $AlCl_3$ + ethylammonium chloride at 90 °C over an extended composition range. The figure shows two regions of composition dependence. The major change at 50 mol % $AlCl_3$ is compared with the corresponding change for the $AlCl_3$ + NaCl system extrapolated to the same temperature. Note that the (EAH)Cl-containing solutions are not only more basic than the corresponding NaCl-containing solutions but are also more acidic for $AlCl_3$ contents greater than 50 mol %.

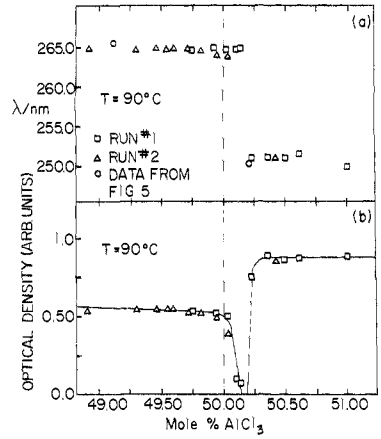

Figure 7. (a) Variation of the absorption maximum for Pb^{2+} in $AlCl_3$ + (EAH)Cl solutions in the immediate vicinity of the equivalence point. Note that the band maximum changes discontinuously across the equivalence point. (b) Variation of the optical density in the same composition region, showing the Pb^{2+} is thrown out of solution in the composition range 50.2–50.4 mol % $AlCl_3$.

NaCl–$AlCl_3$ solutions extrapolated to 90 °C from the plots of Figure 3. It is seen not only that the spectral shift at 90 °C is much greater for (EAH)Cl than for NaCl but also that there is a second, broad region of λ_{max} increase that extends from about 55 to 75 mol % (EAH)Cl, yielding a combined $\Delta\nu$ of 3800 cm^{-1} at 70 mol % (EAH)Cl rising finally to 4400 cm^{-1} by 100 mol % (EAH)Cl. Comparing the Pb^{2+} spectrum in pure (EAH)Cl, ν_{max} = 35 700 cm^{-1}, with the spectrum in the LiCl–KCl eutectic[16] (in which ν_{max} = 36 200 cm^{-1} at 440 °C, implying ~37 900 cm^{-1} at 90 °C), we see that (EAH)Cl behaves in a far more basic manner

than any of the alkali chlorides. Interestingly enough, on the acid side of the equivalence point we find the system containing (EAH)Cl to behave as if more *acidic* than the corresponding alkali chloride containing system. A similar observation has been made, using thermodynamic techniques for the system $AlCl_3$ + *n*-butylpyridinium chloride.[31]

Focusing on the equivalence region, we show two independent titrations in which the composition of the melt was changed in small increments in Figure 7a. A sudden jump in the position of the absorption band maximum, in the absence of any systematic change during the titration, is observed. A plot of optical density (which is proportional to the concentration of the absorbing Pb^{2+} species with the assumption of Beer's Law) vs. mole percent of (EAH)Cl, Figure 7b, shows that the Pb^{2+} ion is thrown out of solution (possibly as $PbCl_2$) in the narrow composition range 49.75 > mol % (EAH)Cl > 49.85. When the titration continues beyond a critical composition, the Pb^{2+} redissolves.

Discussion

As anticipated, the change in Pb^{2+} ion environment from Al^{3+}-polarized chloride ions in $AlCl_3$ to essentially free chloride ions in (EAH)Cl is manifested by a substantial change in 6P ← 6S transition energy, ~4000 cm^{-1}, if we use the insert in Figure 4 to compare at the same temperature. The transition energy in (EAH)Cl is the lowest yet observed in any chloride medium, being 600 cm^{-1} below that in LiCl–KCl at 440 °C[16] (~2180 cm^{-1} below if compared at 90 °C—see Figure 4 insert) and 2100 cm^{-1} below that in $ZnCl_2$ glass at room temperature.[12] The ordering of these shifts reflects the availability of electrons from chloride ions to mix into inner atomic orbitals in the Pb^{2+} electronic structure, i.e., the donor power of the chloride ion environment selected by the Pb^{2+} ions. Since $ZnCl_2$ is regarded as a strong Lewis acid, *its Pb^{2+} band energy in relation to those of $AlCl_3$ + NaCl basic* melts (Figure 4 insert) seems somewhat anomalous. This is perhaps due to the influence of the glass network structure on the Pb^{2+} coordination state.

The spectral shifts are not, and are not expected to be, as great as those observable in oxide systems (e.g.: B_2O_3 glass, 47 200 cm^{-1}; CaO crystal, 29 700 cm^{-1}; $\Delta\nu$ = 17 500 cm^{-1}). However, they have the great advantage, essential to this project, that they can be studied isothermally in the liquid state and can be studied through a well-characterized and very sharp equivalence point.

The changes observed in the latter analytically important region are very sharply defined, though appropriately less so at the higher temperatures (Figure 4). The direct comparison of interest, viz., with the sharpness of the thermodynamic equivalence point, is made in Figure 8, where the composition dependence of $\nu(Pb^{2+})$ is compared with that of pCl from the emf study data of Torsi and Mamantov[22] and the more recent and precise study of Bjerrum and co-workers.[25] The comparison is appropriate since the change in pCl ($=-\log a_{Cl^-} \approx -^1/_2 \log a_{KCl}$), where only the last quantity in the expression in parentheses is well-defined, scales with the free energy change in the reaction; the latter is basically a result of the decrease of electronic potential energy occurring when Cl^- enters the coordination sphere of Al^{3+}. $\Delta\nu$ likewise reflects the change in electronic energy resulting from an exchange of Pb^{2+} nearest neighbors from Cl^- polarized by Al^{3+} to Cl^- otherwise unpolarized; i.e., *it senses the same electronic configuration change that determines most of ΔG for the reaction.* Indeed, the change in the UV excitation energy, 1800 $cm^{-1} \equiv 0.22$ eV, due to the change in chloride environment at the equivalence point is comparable to the change in the chloride ion chemical potential $2.303(RT/F)(\Delta pCl) = 0.57$ eV.

Figure 8 shows that, within the ν_{max} measurement accuracy, the spectroscopically observed energy change and the thermodynamically observed energy changes occur in the same, very narrow, composition range. In this respect Pb^{2+} serves as a rather good *indicator* for the $AlCl_3$ acid titration of the base Cl^-. Its satisfactory character in this respect is further established by

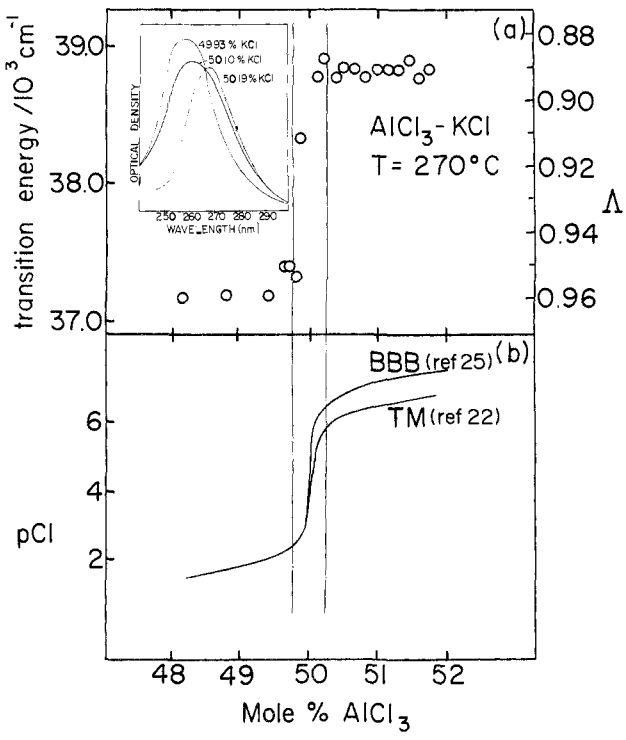

Figure 8. Comparison of the composition interval in which the change in Pb^{2+} absorption maximum occurs (a) with that in which the chloride activity changes according to thermodynamic studies[22,23] (b) in the system KCl + $AlCl_3$. The correspondence confirms that Pb^{2+} can serve as an *accurate indicator for chloride ion activity or, more properly, the alkali* chloride activity, in these melts. The right-hand scale in part a shows the variation of the optical basicities, Λ defined according to eq 1, with composition. The insert shows the Pb^{2+} spectra through the equivalence point with a display of band broadening at 50.1 mol % $AlCl_3$ due to the presence of two distinct Pb^{2+} environments.

considerations, taken up below, of behavior of the Pb^{2+} probe in the basic region. First, however, we should cast the changes in electronic environment of Pb^{2+} that we have described above in more conventional terms. The interaction of the Pb^{2+} species with "otherwise unpolarized" chlorides is usually described by writing a specific chemical species, of which $PbCl_4^{2-}$ would seem the most reasonable choice,[32] and regarding the basic region spectrum as the spectrum of this species. On the acid side of the system, the "species" whose spectrum is observed is a much less obvious entity because of the inferior competition offered by Pb^{2+} vis-à-vis Al^{3+} for the ligands in the system. There is no information available to decide how many Cl^- ions of how many distinct $AlCl_4^-$ species surround and interact with Pb^{2+} at any given instant nor how frequently they are exchanged by rotation or outward displacement. Therefore, while it may be convenient and economical to describe the spectral changes as a consequence of a chemical equilibrium such as

$$Pb(AlCl_4)_n^{n-2} + 4Cl^- \rightarrow PbCl_4^{2-} + nAlCl_4^- \qquad (2)$$

there is, in so doing, some risk of obscuring the physics of the process being studied. This is made more obvious by two considerations, the first of which we consider below and the second of which we reserve for a separate paper except for the following observation.

In the present, and related systems, the same $^3P_1 \leftarrow {}^1S_0$ Rydberg transition in the species Tl^+ does not change in energy in the composition region up to KCl saturation;[33] i.e., it does not behave

(31) J. Robinson and R. A. Osteryoung, *J. Am. Chem. Soc.*, **101**, 323 (1979).

(32) The Raman spectral evidence suggests a tetrahedral $PbCl_4^{2-}$ arrangement (G. N. Papatheodorou, private communications) though the existence of a compound $KPbCl_3$, in which the Pb^{2+} ion is six-coordinated, shows that the preference for tetrahedral coordination in the liquid state is not great and is probably entropy driven.

(33) C. A. Angell and P. D. Bennett, to be submitted for publication.

like Pb^{2+}. Nevertheless, the spectrum has a frequency maximum clearly different from that observed in LiCl–KCl eutectic,[16] even after allowance for temperature change is made. Thus experiments in the system $KAlCl_4$ + LiCl–KCl eutectic would show a spectroscopic shift for which a chemical interpretation would be obliged to invent species of the type $TlCl_n^{(n-1)-}$. But since Tl^+ would, with K^+, be the weakest competitor for ligands in the system, such a description would lack force.

The other consideration concerns the further spectral changes observed in the basic region of the present (EAH)Cl + $AlCl_3$ system (see Figure 6). These changes, which stand as further evidence of the sensitivity of Pb^{2+} as an acid–base indicator in chloride systems, seem unlikely to be due to any change in the first coordination shell of Pb^{2+}; i.e., $PbCl_4^{2-}$ will be present on both sides of any chemical equation we write, and the species-based description will become increasingly cumbersome as the *second* nearest neighbors of the Pb^{2+} species enter the scene. To recognize the new acid–base process being detected, and to guide the writing of the new equilibrium if it is desired, it is helpful to refer to the relevant phase diagrams.

In the composition region of interest to this study, 0–50% $AlCl_3$, the phase diagrams of the $AlCl_3$–NaCl and $AlCl_3$–KCl systems are rather simple.[34] A single congruently melting compound, $M^+AlCl_4^-$, exists in each case. Thus most of the observable change in "chloride ion activity" is expected to occur close to the $AlCl_4^-$ stoichiometry. In the $AlCl_3$ + (EAH)Cl system, however, the existence of a second compound, 2(EAH)Cl + $AlCl_3$, i.e., $[(EAH)_2Cl]^+AlCl_4^-$, of relatively high lattice energy (as indicated by the melting point) suggests the existence of an additional type of interaction in the basic solution range. Such an interaction must be expected to affect the thermodynamic properties although, unfortunately, no suitable thermochemical or chemical potential measurements are yet available to document the magnitude. An estimate, based on NMR chemical shift data for the $AlCl_3$ + pyHCl system,[30] of the free energy of formation of the liquid of the 2:1 compound stoichiometry from pyHCl and $pyHAlCl_4$ yielded the value ~50 kJ mol^{-1}, far in excess of RT at the temperature of this study. This should produce an (EAH)Cl activity change of about 2 orders of magnitude, which an appropriate indicator should easily detect. From the general similarity of the $AlCl_3$–(EAH)Cl and $AlCl_3$–pyHCl phase diagrams,[29] particularly the curvatures of the liquidus lines, similar changes are anticipated in the present system.

The findings of the present study in the composition regions 0–50 mol % $AlCl_3$ are clearly consistent with the above considerations, permitting the qualitative conclusion that Pb^{2+} is a sensitive, wide-range, indicator for all the Cl^- acid–base reactions in these systems. Furthermore—and this is important—*it is an indicator that can distinguish between, and perhaps ultimately quantify systematically, the differences in the absolute basicities of different bases.* This can be seen from the different λ_{max} values on the basic sides of Figures 5 and 6. For an association of numerical values with the spectral changes observed in the KCl + $AlCl_3$ system, the Duffy–Ingram optical basicities, Λ, obtained by using eq 1, are included in Figure 8a, rhs scale.

It is notable, though, that in the case of Bi^{3+} and Tl^+, both of which exhibit the same Rydberg transition, very different results are obtained. Tl^+ as mentioned above, shows no λ_{max} changes at the equivalence point while Bi^{3+} shows changes at 50% KCl and 50% (EAH)Cl but it insensitive in the range 50–68% (EAH)Cl (cf. Pb^{2+} in Figure 6). These results, which will be described in more detail in a separate paper,[33] help place the $d^{10}s^2$ cations in perspective as basicity indicators. They are evidently susceptible to the same limitations as afflict conventional aqueous acid–base indicators, viz., the basicity of the indicator must be suitably placed within the range of the process being studied. In the present instance Bi^{3+} is too strongly acid to respond to the minor changes seen by Pb^{2+} in Figure 6, while Tl^+ is too weakly acid to detect the abrupt changes at 50% $AlCl_3$.

The attempt to obtain detailed spectroscopic data for Pb^{2+} in the range of rapid activity change, which would permit more stringent and precise comparisons of thermodynamic and optical basicities, was frustrated by the precipitation of the probe ion, notwithstanding its minute ~10^{-4} M concentration, as shown in Figure 7. This does not occur in the case of Bi^{3+}, which will be discussed in a separate publication.[33] (The apparent 0.2% $AlCl_3$ displacement of the jump in Figure 7 from the exact 1:1 stoichiometry is probably an artifact arising from the introduction of traces of moisture during the many composition changes. Water reacts with the solution to form oxidic species such as $AlOCl_2^-$, increasing the effective free chloride ion concentration so long as the liberated HCl remains trapped (as HCl_2^-[29]) in solution.)

The fact that, in Figure 7, no change whatever occurs in the peak energy in the composition region just before precipitation implies that at no stage in the titration does Pb^{2+} experience an environment in which there is a single unpolarized Cl^- (i.e., with next nearest neighbor EAH^+) amongst the Al^{3+}-polarized Cl^- ions (i.e., $AlCl_4^-$) that comprise the remainder of the coordination shell. Such an environment would be labeled "$PbCl^+$" in normal terminology. Pb^{2+} so coordinated would be expected to yield a red-shifted spectrum. Evidently the solubility product of $PbCl_2$ is exceeded before the population of "$PbCl^+$" is large enough to affect the spectrum (the latter must always be an average of the spectra assignable to individual environments). This implies, at least, that there is no marked chemical stability associated with the "$PbCl^+$" species in the lower temperature melt.

By contrast, in the higher temperature $AlCl_3$ + KCl solutions, the Pb^{2+} remains in solution in this critical composition region of the higher temperature melt (T = 270 °C vs. T = 90 °C for $AlCl_3$ + (EAH)Cl), allowing the observation of its spectrum (see insert to Figure 8a). The *broadened* spectrum for the point at 50.10 mol % $AlCl_3$ demonstrates that the Pb^{2+} in this melt is distributed between the acidic region and basic region Pb^{2+} environments rather than sampling a single intermediate environment; i.e., a two-species or multispecies equilibrium exists, as eq 2 would imply.

Returning to the $AlCl_3$–(EAH)Cl system, we note the invariance of λ_{max} with composition on the basic side of the equivalence point in Figure 7. This suggests a preferred environment exists for the Pb^{2+} ions in the first basic region also, 48–50% $AlCl_3$, though the conformation cannot be judged from the spectra without further information.[32] The further shift in the $AlCl_3$ + (EAH)Cl system that occurs between 0 and 49% $AlCl_3$ could represent simply a replacement, at constant coordination number, of Cl^- doubly polarized by EAH^+ cations (i.e., Cl^- from [EAH–Cl–EAH]$^+$ groups) by Cl^- singly polarized by EAH^+ cations.

Acknowledgment is made to the National Science Foundation, Solid State Chemistry Division, for support of this work under Grant No. DMR 77-04318A1. We are grateful to Drs. M. D. Ingram and L. Boehm for a number of stimulating discussions.

(34) W. Fischer and A. Simon, *Z. Anorg. Allg. Chem.*, **306**, 1 (1960).

Registry No. Pb^{2+}, 14280-50-3; $AlCl_3$, 7446-70-0; (EAH)Cl, 557-66-4.